

Klein-Nishina effect and the cosmic ray electron spectrum

Kun, Fang^a, Xiao-Jun Bi^{a,b,*}, Su-Jie Lin^c, and Qiang Yuan^{d,e,f†}

^a*Key Laboratory of Particle Astrophysics,
Institute of High Energy Physics,
Chinese Academy of Science,
Beijing 100049, China*

^b*University of Chinese Academy of Sciences,
Beijing 100049, China*

^c*School of Physics and Astronomy,
Sun Yat-Sen University,
Zhuhai 519082, GuangDong, China*

^d*Key Laboratory of Dark Matter and Space Astronomy,
Purple Mountain Observatory,
Chinese Academy of Sciences,
Nanjing 210033, China*

^e*School of Astronomy and Space Science,
University of Science and Technology of China,
Hefei, Anhui 230026, China*

^f*Center for High Energy Physics,
Peking University, Beijing 100871, China*

(Dated: July 31, 2020)

Abstract

Radiative energy losses are very important in regulating the cosmic ray electron spectrum during their propagation in the Milky Way. Particularly, the Klein-Nishina (KN) effect of the inverse Compton scattering (ICS) results in less efficient energy losses of high-energy electrons, which is expected to leave imprints on the propagated electron spectrum. It has been proposed that the spectral hardening of cosmic ray electron (or electron plus positron) spectra around 50 GeV observed by Fermi-LAT, AMS-02, and DAMPE might be due to the KN effect. We show in this work that the transition from the Thomson regime to the KN regime of the ICS is actually quite smooth. As a result, the expected hardening feature due to the KN loss is less significant. To account for the features of the spectra of cosmic ray electrons and positrons, an additional hardening of the primary electron spectrum is needed. We also provide a parameterized form for the precise calculation of the ICS energy loss rate in a wide energy range.

* bixj@mail.ihep.ac.cn

† yuanq@pmo.ac.cn

I. INTRODUCTION

Precise measurements of the energy spectra of cosmic ray electrons and/or positrons (CREs) have achieved big progresses in recent years [1–10], which are very important in probing the origin and propagation of CREs, as well as new physics such as the dark matter annihilation. Several features have been shown in the energy spectra of CREs, including a softening around several GeV [4, 5], a hardening at ~ 50 GeV [6, 8, 9], and a softening again at $E \sim 0.9$ TeV [2, 6]. It is interesting to note that before the direct detection of the spectral hardening at ~ 50 GeV such a feature has been indicated by fitting to the AMS-02 positron fraction and electron plus positron data [11–14]. These features have interesting and important implications on the origin of CREs. Together with the positron excesses [15, 16], a three-component scenario of electrons and positrons is generally established, which includes the *primary electrons* accelerated simultaneously with nuclei, the *secondary electrons and positrons* produced by the inelastic collisions between cosmic ray nuclei and the interstellar medium, and the *additional electrons and positrons* contributing to the high-energy excesses (see e.g., [17]).

One prominent effect of the CRE propagation in the Milky Way is the energy loss, due to the ionization and Coulomb scattering ($\dot{E} \propto \text{const.}$), the bremsstrahlung radiation ($\dot{E} \propto E$), and the synchrotron and inverse Compton scattering (ICS) radiation ($\dot{E} \propto E^2$). For typical parameters of the Milky Way, the synchrotron and ICS energy-losses are dominant for CREs with energies \gtrsim GeV [18, 19]. However, the E^2 form of the energy-loss rate for the ICS process is only valid in the Thomson regime, when $4E\epsilon/(m_e c^2)^2 \ll 1$, where ϵ is the energy of the target photon, and m_e is the mass of electron. At higher energies (either the CRE or the target photon has a high enough energy), the ICS cross section takes the full Klein-Nishina (KN) form, which gets suppressed compared with the Thomson cross section, resulting in a smaller energy-loss rate. The KN effect is expected to be important even for CREs below TeV energies, from the scattering with the ultraviolet-optical and infrared components of the interstellar radiation field (ISRF). The reduction of the ICS loss rate is expected to give higher equilibrium CRE fluxes, leaving hardening features on the CRE spectrum [20]. This effect has been employed to explain the ~ 50 GeV hardening of the CRE spectrum [21, 22].

Previous studies usually adopt the simple analytical approximation of the KN loss [21–23]. Here we show that considering the precise form of the KN cross section of the ICS, the

transition from the Thomson regime to the KN regime becomes much smoother, and thus the hardening effect on the CRE spectrum due to the KN loss is less distinct. Taking the realistic ISRF distribution in the Milky Way into account, our results show that the observed spectral hardening of the CRE spectrum at ~ 50 GeV by Fermi-LAT, AMS-02, and DAMPE should not be solely due to the KN loss effect. A parameterized form to describe the precise ICS energy-loss rate valid from the Thomson limit to the extreme KN limit has also been provided.

II. ENERGY-LOSS RATE OF THE INVERSE COMPTON SCATTERING

Due to the efficient radiative energy losses, high energy CREs can only travel a short distance in the Milky Way. Typically for CREs above ~ 1 GeV, the energy-loss effect dominates over the escape effect and becomes essential for the spectral shape of the propagated CREs. Synchrotron radiation and ICS dominate the energy losses of the high-energy CREs. If the energy dependency of the energy-loss rate has a power-law form just like the synchrotron loss, the high-energy electron spectrum can also be written as a power law given a homogeneously distributed source term [24, 25]. However, for the ICS, the KN suppression of the cross section leads to correction of the conventional E^2 form of the energy-loss rate in the Thomson limit. As a result, the propagated CRE spectrum should also deviated from a simple power-law, as have been studied in many works [21–25].

Using the Lorentz factor $\gamma = E/(m_e c^2)$ as variable, the ICS energy-loss rate of a single electron with energy E can be written as [23]

$$|\dot{\gamma}|_{\text{ic}} = \frac{12c\sigma_T\gamma^2}{m_e c^2} \int_0^\infty d\epsilon \epsilon n(\epsilon) \int_0^1 dq \frac{qF(\Gamma, q)}{(1 + \Gamma q)^3}, \quad (1)$$

where σ_T is the Thomson cross section, ϵ is the energy of the target photon, $n(\epsilon)$ is the energy distribution of an isotropic photon field, $\Gamma = 4\epsilon\gamma/(m_e c^2)$, and

$$F(\Gamma, q) = 2q \ln q + (1 + 2q)(1 - q) + \frac{(\Gamma q)^2(1 - q)}{2(1 + \Gamma q)}, \quad (2)$$

which is derived from the exact KN formula [20, 26].

For electrons propagating in the Milky Way, the target photon field includes the ISRF and the cosmic microwave background (CMB). We adopt the local ISRF provided in [25], which consists of five gray-body components, with temperatures of 23209.0 K, 6150.4 K,

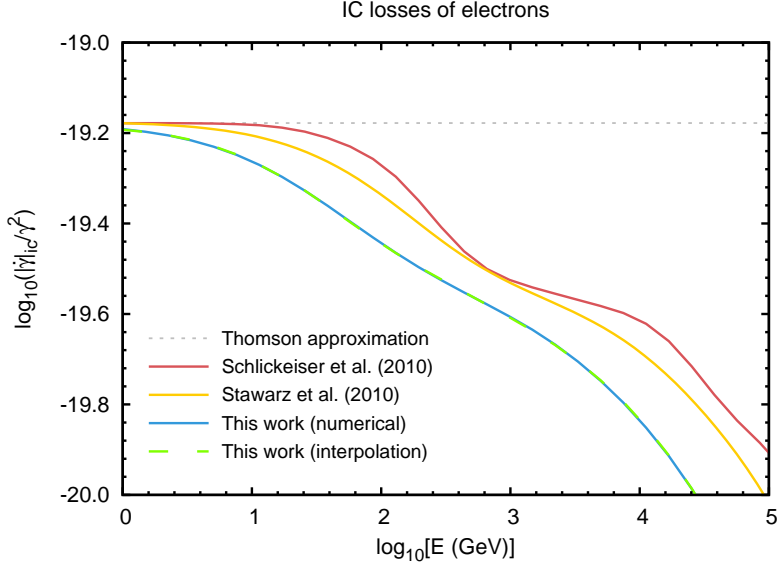


FIG. 1. Electron energy-loss rates due to the ICS. The blue solid line shows the numerical integration of Eq. (1), and the green dashed line is obtained from the parameterization of Eq. (5). For comparison, we show the results of the Thomson regime in gray dotted line, and of the approximations in Refs. [21, 23] in orange and red solid lines. For all cases the ISRF is taken from Ref. [25].

3249.3 K, 313.3 K, 33.1 K, and energy densities of 0.12 eV cm^{-3} , 0.23 eV cm^{-3} , 0.37 eV cm^{-3} , 0.055 eV cm^{-3} , 0.25 eV cm^{-3} , respectively. The temperature and energy density of the CMB are 2.725 K and 0.26 eV cm^{-3} [27].

We show the exact ICS loss rate from a numerical integration of Eq. (1) in Fig. 1 with the blue solid line. Compared with the result computed in the Thomson limit, the KN effect starts to appear for $E \gtrsim \text{GeV}$, for the Milky Way ISRF. We also compare the results from various approximations of the KN loss in literature [21, 23]. It is shown that there are relatively large differences of those approximations from the numerical computation. Particularly, the numerical result shows less prominent features due to the KN scattering off different ISRF components. This may be due to that the transition from the Thomson regime to the extreme KN regime is actually broader and shallower than those approximations.

Eq. (1) needs a two-dimensional numerical integration, and is inconvenient for general-purpose use. We therefore try to find a proper parameterized approximation of the exact result. For a gray-body photon field with temperature T and energy density w , Eq. (1) can

TABLE I. Coefficients of the interpolating polynomial in Eq. (5).

c_0	c_1	c_2	c_3
-3.996×10^{-2}	-9.100×10^{-1}	-1.197×10^{-1}	3.305×10^{-3}
c_4	c_5	c_6	
1.044×10^{-3}	-7.013×10^{-5}	-9.618×10^{-6}	

be rewritten as

$$|\dot{\gamma}|_{\text{ic}} = \frac{20c\sigma_T w \gamma^2}{\pi^4 m_e c^2} Y(\gamma, T), \quad (3)$$

where

$$Y(\gamma, T) = \frac{9}{(kT)^4} \int_0^\infty d\epsilon \frac{\epsilon^3}{\exp[\epsilon/(kT)] - 1} \int_0^1 dq \frac{qF(\Gamma, q)}{(1 + \Gamma q)^3}, \quad (4)$$

with k being the Boltzmann constant. Setting $x = 4\gamma kT/(m_e c^2)$, we can easily find that the integral Eq. (4) depends only on variable x . It means that for a gray-body photon field, there is a degeneracy between γ and T for the computation of the ICS loss rate. It is evident that $x \ll 1$ corresponds to the Thomson regime, while $x \gg 1$ corresponds to the extreme KN regime. We find that for $x < 1.5 \times 10^{-3}$ and $x > 150$, $Y(x)$ can be respectively approximated by the analytical formulae in the Thomson and the KN limits within an accuracy better than 1%. In the intermediate regime, we use a six-order polynomial function in the log-log space to describe $Y(x)$. Then we obtain the expression of $Y(x)$ in the whole range as

$$Y(x) = \begin{cases} \frac{\pi^4}{15} & x \leq 1.5 \times 10^{-3} \\ \exp \left[\sum_{i=0}^6 c_i (\ln x)^i \right] & 1.5 \times 10^{-3} < x < 150 \\ \frac{3}{4} \left(\frac{\pi}{x} \right)^2 (\ln x - 1.9805) & x \geq 150 \end{cases}. \quad (5)$$

This approach ensures an accuracy of 1% in the whole energy range. The coefficients of the polynomial function are listed in Table I. The ICS loss rate calculated with Eq. (5) is also shown in Fig. 1, which is well consistent with the numerical calculation.

III. IMPACT ON THE ELECTRON SPECTRUM

Before calculating the CRE spectrum, we discuss the first derivative of the energy-loss rate, i.e., the spectral index of the energy-loss rate. This quantity directly reflects the

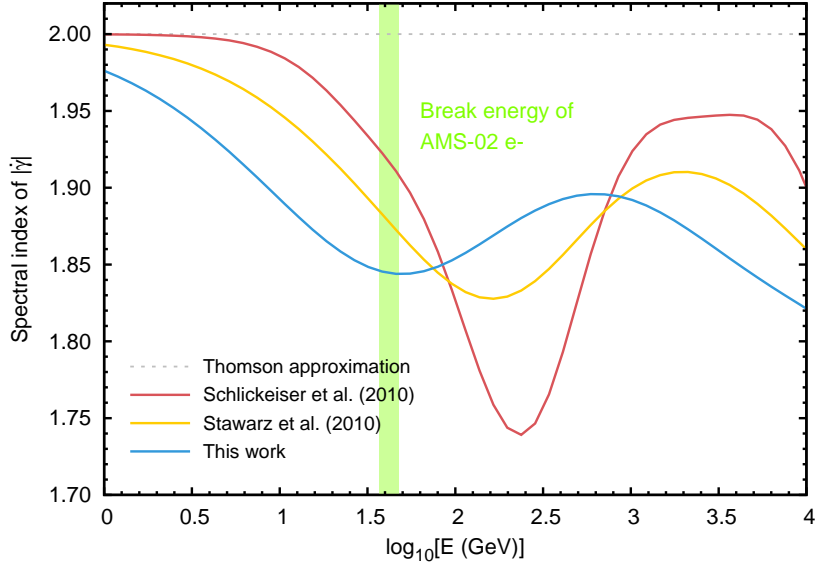


FIG. 2. First derivative of the radiative loss rate (with both synchrotron and ICS losses) verse electron energy. This quantity reflects the impact on the primary electron spectrum due to the radiative loss. The blue line is obtained in this work, and the red line is from Ref. [22]. The green band shows the break energy (1σ confidence interval) of the electron spectrum measured by AMS-02 [9].

impact on the primary electron spectrum due to the radiative losses. The total loss rate for high-energy CREs is $|\dot{\gamma}| = |\dot{\gamma}|_{\text{ic}} + |\dot{\gamma}|_{\text{syn}}$, where $|\dot{\gamma}|_{\text{syn}}$ is the synchrotron loss rate:

$$|\dot{\gamma}|_{\text{syn}} = \frac{\sigma_T c B^2 \gamma^2}{6\pi m_e c^2}. \quad (6)$$

We take $B = 3 \mu\text{G}$ as a benchmark interstellar magnetic field strength.

Fig. 2 shows the spectral indices of $|\dot{\gamma}|$ calculated in this work and in Ref. [22]. It shows that the KN effect indeed results in complicated spectral changes which would imprint on the final CRE spectrum. However, different approaches of the KN loss give different quantitative features.

The latest measurement of the electron spectrum by AMS-02 indicates a spectral hardening at $\sim 42.1 \text{ GeV}$ [10]. Ref. [22] proposed that this hardening feature can be understood as the decrease of the ICS loss rate due to the KN effect on the ultraviolet-optical backgrounds. However, as shown in Fig. 2, the KN effect actually appears at even earlier energies ($\sim \text{GeV}$). The spectral index of $|\dot{\gamma}|$ keeps decreasing to about 40 GeV, and then increase for

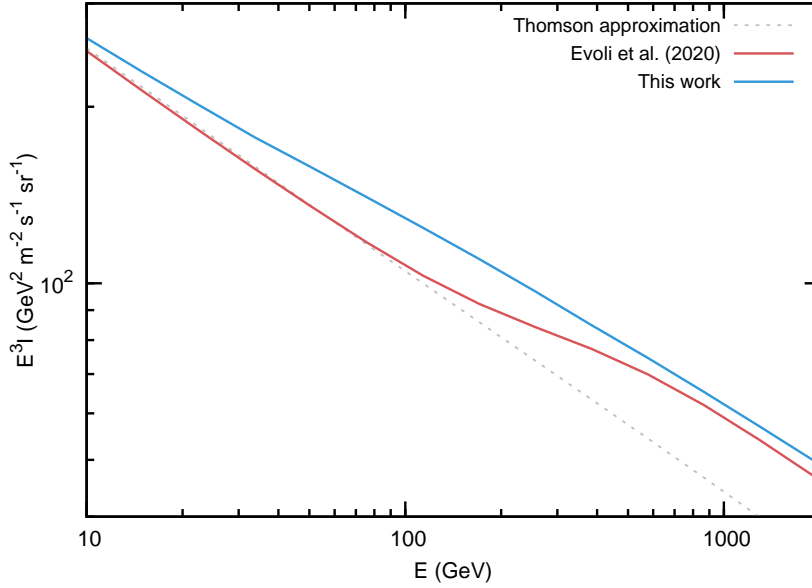


FIG. 3. Primary electron fluxes after including the synchrotron and ICS energy-loss effects. The injection spectral index is set to be 2.7, and the normalization of the injection spectrum is set to be 10^{51} GeV^{-1} . The red solid line is obtained with the ICS loss rate used in [22], while the blue solid line is calculated with the accurate IC loss rate in the present work.

$E \gtrsim 40 \text{ GeV}$. It means that the electron spectrum should become softer other than being harder at 40 GeV.

The propagation of CREs in the ISM can be described by the diffusion-energy-loss equation:

$$\frac{\partial N}{\partial t} - D\Delta N + \frac{\partial}{\partial E}(bN) = Q(E, \mathbf{x}, t), \quad (7)$$

where $N(E)$ is the differential number density of CREs, $D(E)$ is the diffusion coefficient, $b(E) = \dot{\gamma}m_e c^2$ is the energy-loss rate, and $Q(E, \mathbf{x}, t)$ is the source function. The diffusion coefficient is adopted as $D(E) = 3.67 \times 10^{28} (E/1 \text{ GeV})^{0.33}$, which is consistent with the B/C measurements (e.g., [28]). We assume a power-law injection spectrum for the source term as $Q \propto E^{-\alpha}$. Since supernova remnants (SNRs) are widely believed to be the main source of primary cosmic rays, we adopt the spatial distribution of SNRs given in Ref. [29] as the source function. The Galactic supernova explosion rate is assumed to be 3 per century.

We find the stationary solution of Eq. (7) using the Green's function method. A cylinder geometry of the diffusion zone is assumed. The half-height of the cylinder is set to be 5 kpc [28]. One may refer to Ref. [25] for details of the Green's function. The calculated

primary electron spectra are given in Fig. 3. Here we show the results with the Thomson approximation of the ICS loss rate (gray dotted line), the ICS loss rate approximation adopted in Ref. [22], and the parameterization of Eq. (5) in this work. We can see that although the inclusion of the KN effect shows remarkable difference from the Thomson approximation of the ICS, no prominent feature of the propagated electron spectrum can be obtained if we only consider the energy-loss effect. Therefore we expect that the spectral hardening of the CRE spectra should be originated from other effects than the propagation, e.g., the source effect.

The proportion of the synchrotron component in the energy-loss term may also affect the spectral features of CREs, as pointed out by Ref. [30]. Given the typical magnetic field strength of the Milky Way, the synchrotron loss may only be important at much higher energies (for example, ~ 10 TeV).

IV. CONCLUSION AND DISCUSSION

The radiative energy loss of electrons and positrons is crucial to determining the spectra of CREs during the propagation. Due to the KN effect of the ICS, the primary electron spectrum is expected to deviate from simple power-law form even if the accelerated spectrum is a power-law. We find that the KN effect does affect the propagated electron spectrum, compared with the Thomson approximation of the ICS. However, the transition from the Thomson regime to the KN regime is relatively broad and shallow, and hence no prominent spectral feature of the electron spectrum is expected before a few TeV. We note that in some works the approximation of the ICS energy-loss rate in the intermediate range between the Thomson and KN limits is less precise, which may give distinct spectral features of the electron spectrum. For the convenience of practical use, we further give a polynomial form to describe the ICS loss rate in the intermediate region between the Thomson and extreme KN limits.

Our result shows that the spectral hardening of the CREs at ~ 50 GeV found by several experiments should not be entirely due to the KN energy-loss effect. The source of the positron anomaly may contribute partly to this spectral hardening. Besides the extra positron and electron source, the simultaneous fit to the CRE spectra and the positron fraction further suggests a spectral hardening of the primary electron spectrum at several tens

of GeV [11–14]. Physically the origin of the spectral hardening may be due to the discrete distribution of cosmic ray acceleration sources (e.g., [31–34]).

ACKNOWLEDGMENTS

This work is supported by the National Key Research and Development Program of China (No. 2016YFA0400203, 2016YFA0400204), the National Natural Science Foundation of China (Nos. 11722328, U1738205, 11851305), the 100 Talents program of Chinese Academy of Sciences, and the Program for Innovative Talents and Entrepreneur in Jiangsu.

-
- [1] J. Chang, J. H. Adams, H. S. Ahn, *et al.*, *Nature* **456**, 362 (2008).
 - [2] F. Aharonian, A. G. Akhperjanian, U. Barres de Almeida, *et al.*, *Phys. Rev. Lett.* **101**, 261104 (2008), arXiv:0811.3894 [astro-ph].
 - [3] A. A. Abdo, M. Ackermann, M. Ajello, *et al.*, *Phys. Rev. Lett.* **102**, 181101 (2009), arXiv:0905.0025 [astro-ph.HE].
 - [4] O. Adriani, G. C. Barbarino, G. A. Bazilevskaya, *et al.*, *Phys. Rev. Lett.* **106**, 201101 (2011), arXiv:1103.2880 [astro-ph.HE].
 - [5] M. Aguilar, D. Aisa, B. Alpat, *et al.*, *Phys. Rev. Lett.* **113**, 221102 (2014).
 - [6] G. Ambrosi, Q. An, R. Asfandiyarov, *et al.*, *Nature* **552**, 63 (2017), arXiv:1711.10981 [astro-ph.HE].
 - [7] O. Adriani, Y. Akaike, K. Asano, *et al.*, *Phys. Rev. Lett.* **119**, 181101 (2017), arXiv:1712.01711 [astro-ph.HE].
 - [8] S. Abdollahi, M. Ackermann, M. Ajello, *et al.*, *Phys. Rev. D* **95**, 082007 (2017), arXiv:1704.07195 [astro-ph.HE].
 - [9] M. Aguilar, L. Ali Cavazonza, G. Ambrosi, *et al.*, *Phys. Rev. Lett.* **122**, 041102 (2019).
 - [10] M. Aguilar, L. Ali Cavazonza, B. Alpat, *et al.*, *Phys. Rev. Lett.* **122**, 101101 (2019).
 - [11] Q. Yuan and X.-J. Bi, *Physics Letters B* **727**, 1 (2013), arXiv:1304.2687 [astro-ph.HE].
 - [12] I. Cholis and D. Hooper, *Phys. Rev. D* **88**, 023013 (2013), arXiv:1304.1840 [astro-ph.HE].
 - [13] S.-J. Lin, Q. Yuan, and X.-J. Bi, *Phys. Rev. D* **91**, 063508 (2015), arXiv:1409.6248 [astro-ph.HE].

- [14] X. Li, Z.-Q. Shen, B.-Q. Lu, *et al.*, Physics Letters B **749**, 267 (2015), arXiv:1412.1550 [astro-ph.HE].
- [15] O. Adriani, G. C. Barbarino, G. A. Bazilevskaya, *et al.*, Nature **458**, 607 (2009), arXiv:0810.4995 [astro-ph].
- [16] M. Aguilar, G. Alberti, B. Alpat, *et al.*, Phys. Rev. Lett. **110**, 141102 (2013).
- [17] Q. Yuan and L. Feng, Science China Physics, Mechanics, and Astronomy **61**, 101002 (2018), arXiv:1807.11638 [astro-ph.HE].
- [18] A. M. Atoyan, F. A. Aharonian, and H. J. Völk, Phys. Rev. D **52**, 3265 (1995).
- [19] A. W. Strong and I. V. Moskalenko, Astrophys. J. **509**, 212 (1998), arXiv:astro-ph/9807150 [astro-ph].
- [20] G. R. Blumenthal and R. J. Gould, Reviews of Modern Physics **42**, 237 (1970).
- [21] L. Stawarz, V. Petrosian, and R. D. Blandford, Astrophys. J. **710**, 236 (2010), arXiv:0908.1094 [astro-ph.GA].
- [22] C. Evoli, P. Blasi, E. Amato, and R. Aloisio, arXiv e-prints , arXiv:2007.01302 (2020), arXiv:2007.01302 [astro-ph.HE].
- [23] R. Schlickeiser and J. Ruppel, New Journal of Physics **12**, 033044 (2010), arXiv:0908.2183 [astro-ph.HE].
- [24] T. Kobayashi, Y. Komori, K. Yoshida, and J. Nishimura, Astrophys. J. **601**, 340 (2004), arXiv:astro-ph/0308470 [astro-ph].
- [25] T. Delahaye, J. Lavalle, R. Lineros, F. Donato, and N. Fornengo, Astron. Astrophys. **524**, A51 (2010), arXiv:1002.1910 [astro-ph.HE].
- [26] F. C. Jones, Physical Review **167**, 1159 (1968).
- [27] D. J. Fixsen, Astrophys. J. **707**, 916 (2009), arXiv:0911.1955 [astro-ph.CO].
- [28] Q. Yuan, S.-J. Lin, K. Fang, and X.-J. Bi, Phys. Rev. D **95**, 083007 (2017), arXiv:1701.06149 [astro-ph.HE].
- [29] D. A. Green, Mon. Not. Roy. Astron. Soc. **454**, 1517 (2015), arXiv:1508.02931 [astro-ph.HE].
- [30] F. A. Agaronian and A. S. Ambartsumyan, Astrophysics **23**, 650 (1985).
- [31] C. S. Shen, Astrophys. J. Lett. **162**, L181 (1970).
- [32] F. A. Aharonian, A. M. Atoyan, and H. J. Voelk, Astron. Astrophys. **294**, L41 (1995).

- [33] M. Di Mauro, F. Donato, N. Fornengo, R. Lineros, and A. Vittino, *J. Cosmol. Astropart. Phys.* **2014**, 006 (2014), arXiv:1402.0321 [astro-ph.HE].
- [34] K. Fang, B.-B. Wang, X.-J. Bi, S.-J. Lin, and P.-F. Yin, *Astrophys. J.* **836**, 172 (2017), arXiv:1611.10292 [astro-ph.HE].